Building Robust Classifiers with Generative Adversarial Networks for Detecting Cavitation in Hydraulic Turbines

Andreas Look, Oliver Kirschner and Stefan Riedelbauch
Institut für Strömungsmechanik und Hydraulische Strömungsmaschinen, Universität Stuttgart, 70565 Stuttgart, Germany

Keywords: Convolutional Neural Networks, Generative Networks, Condition Monitoring.

Abstract: In this paper a convolutional neural network (CNN) with high ability for generalization is build. The task of the network is to predict the occurrence of cavitation in hydraulic turbines independent from sensor position and turbine type. The CNN is directly trained on acoustic spectrograms, obtained form acoustic emission sensors operating in the ultrasonic range. Since gathering training data is expensive, in terms of limiting accessibility to hydraulic turbines, generative adversarial networks (GAN) are utilized in order to create fake training data. GANs consist basically of two parts. The first part, the generator, has the task to create fake input data, which ideally is not distinguishable form real data. The second part, the discriminator, has the task to distinguish between real and fake data. In this work an Auxiliary Classifier-GAN (AC-GAN) is build. The discriminator of an AC-GAN has the additional task to predict the class label. After successful training it is possible to obtain a robust classifier out of the discriminator. The performance of the classifier is evaluated on separate validation data.

1 INTRODUCTION

Cavitation occurs in liquids when pressure locally drops below vapour pressure. When such created vapour bubbles enter regions of higher pressure, they will implode. This implosion can cause damage, if the implosion happens near solid surfaces. The process of nucleation, growth, and implosion is called cavitation (Koivula, 2000).

In hydraulic turbines cavitation mostly occurs when operating close to the limits of the operating range. Often it is not clearly known whether the machinery is currently operating under cavitation conditions or not. It would be advantageous to detect cavitation while the turbines are running, thus the operator can take actions in order to avoid it.

Since visual inspection of cavitation events in hydro power plants is not possible, due to missing optical accessibility, acoustic event detection offers an alternative. Most existing cavitation detecting methods rely on statistically analyzing the radiated noise, i.e. calculating energy content in specific frequency ranges, kurtosis, and other hand crafted features. Afterwards these features are examined by an expert (Escaler et al., 2006) or fed into a classifier, e.g. SVM (Gregg et al., 2017). These methods yield good results in laboratory environment. Representable performance measurements under non laboratory conditions are not available or show a dependency on the sensor location (Schmidt et al., 2014). Therefore in this work a robust model for detecting cavitation is trained and evaluated. Here, robustness means, that there is no dependency on turbine type and no or little dependency on sensor location.

2 HARDWARE SETUP

Cavitation typically radiates noise in a broad frequency range from several Hz up to the ultrasonic range. Analyzing signals containing only information in the ultrasonic range has the advantage of mostly noise free signals. Noise free means, almost no influence from bearings or other mechanical parts. On the other hand the sampling frequency has to be very high and a lot of information has to be processed, which results in long and difficult training.

The radiated noise is recorded by acoustic emission sensors operating in the frequency range between 100 kHz and 1 MHz. Below 100 kHz the sensors behave like highpass filters. The upper frequency bound is limited by the maximum sampling frequency of 2 MHz.

Look, A., Kirschner, O. and Riedelbauch, S.
Building Robust Classifiers with Generative Adversarial Networks for Detecting Cavitation in Hydraulic Turbines.
DOI: 10.5220/0006636304560462
In *Proceedings of the 7th International Conference on Pattern Recognition Applications and Methods (ICPRAM 2018)*, pages 456-462
ISBN: 978-989-758-276-9

Table 1: Architecture of neural network used for conventional training. BN? indicates whether batch normalization (Ioffe and Szegedy, 2015) was used.

Operation	Kernel	Strides	Feature maps	BN?	Dropout	Nonlinearity
Input	N/A	N/A	N/A	N/A	N/A	N/A
Convolution	3×3	1×1	8	$\times$	0.2	ReLu
Max-Pooling	2×2	2×2	8	$\times$	$\times$	N/A
Convolution	3×3	1×1	16	$\times$	0.2	ReLu
Max-Pooling	2×2	2×2	16	$\times$	$\times$	N/A
Convolution	3×3	1×1	32	$\times$	0.2	ReLu
Max-Pooling	2×2	2×2	32	$\times$	$\times$	N/A
Flatten	N/A	N/A	N/A	$\times$	$\times$	N/A
Dense	N/A	N/A	64	$\times$	0.2	ReLu
Dense	N/A	N/A	32	$\times$	$\times$	ReLu
Dense	N/A	N/A	1	$\times$	$\times$	Sigmoid

3 CLASSIFICATION SYSTEM

Basically it is possible to build a classifier, which processes one-dimensional (raw signal) or two-dimensional (spectrograms) data. Convolutional networks are often the best or among the best performing neural networks in acoustic scene classification challenges (Mesaros et al., 2017; Stowell et al., 2016). Moreover CNNs are well studied in various condition monitoring applications and are usually more often chosen (Zhao et al., 2016). Since CNNs are originally designed for image recognition tasks, a two-dimensional representation of the data is used.

All experiments in this work were done using Tensorflow (Abadi et al., 2015).

3.1 Data Preprocessing

Before the data is used for training a classifier it has to be preprocessed. The first step consists of applying short-time fourier transformation (STFT) and building spectrograms with size 512×384 (*Frequency* $\times$ *Time*). The STFT uses a Hanning window and 50 % overlap. Thus approximately every 0,1 s one spectrogram is obtained. Since a wide frequency range shall be analyzed, dynamic range compression (DCR) (Lukic et al., 2016) is used in order to reduce the dynamics between high and low frequencies.

$$f(x_{ij}) = \log(1 + C \cdot x_{ij}) \tag{1}$$

DCR corresponds to the elementwise application of function 1 on every element x_{ij} in a spectrogram with $C = 10^{12}$. C is empirically set and will not be changed in the course of this work. For dimensional reduction the frequency axis is wrapped by a filter bank, which consists of 32 equally spaced and non overlapping triangular windows. This method is inspired by creating Mel-frequency cepstral coefficients, which have proven robustness in several audio recognition tasks (Sahidullah and Saha, 2012). After wrapping, spectrograms with reduced size $32x384$ are obtained.

3.2 Conventional Training

Table 1 shows the network used for conventional training. Conventional training in this context means, no usage of synthetic data. The network consists of three dense layers and three convolutional layers.

Before every layer, except the last one, dropout (Srivastava et al., 2014) is applied in order to improve the generalization capability. Additionaly after convolution max-pooling with kernel size 2×2 and stride 2×2 is followed. Since the task is to detect whether cavitation occurs in the spectrogram or not, max-pooling is useful. Basically it represents a strong prior, stating that the occurrence of cavitation is independent of the position in the spectrogram (Goodfellow et al., 2016). The kernel size of the convolutional layers is 3×3 with stride 1×1. In the first layer 8 filters, in the second 16 filters, and the third layer 32 filters are used. The network is trained using the Adam optimizer with a learning rate of 10^{-3} and batch size 16 for 40.000 weight updates, corresponding to 70 epochs. Since the task is a classification task, cross entropy is used as loss function.

Figure 1 shows the learning curve. The whole dataset consists of five different hydraulic turbines. For training purposes measurements from four different turbines are used. Measurements from the fifth turbine are part of the validation dataset. Therefore the validation dataset consists of completely unknown

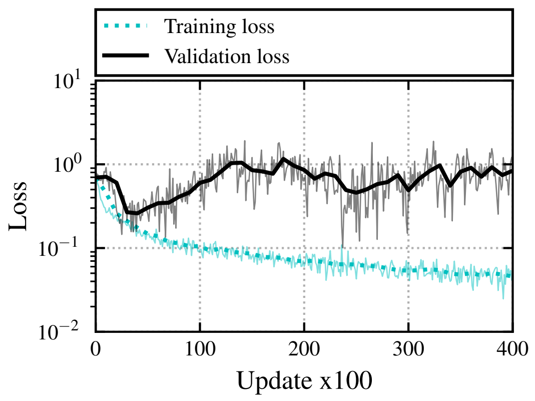

Figure 1: Learning curve of conventional architecture.

positions and turbine configurations. The validation dataset consists of four different sensor positions and has a 50/50 split between cavitation and no cavitation.

According to the learning curve the training loss decreases continuously. At the beginning of the training the validation loss also sinks, but already shortly after rises and then stagnates. The binary accuracy of the validation dataset at the end of the training is $80,1 \pm 2,5\,\%$. The accuracy is estimated by evaluating the validation dataset 64 times with dropout and afterwards calculating the mean and standard deviation (Gal and Ghahramani, 2015). With early stopping after 3500 weight updates (minimal validation loss) a binary accuracy of $94,2 \pm 2,0\,\%$ is obtained.

Increasing dropout rate or adding additional noise to the inputs and hidden layers respectively often represent potential solutions for further increasing generalization capability, but did not succeed in this case.

3.3 Generative Adversarial Networks

Generative adversarial networks (GAN) (Goodfellow et al., 2014) consist of two competing neural networks, a generator (G) and a discriminator (D). G takes as input random noise and outputs fake data, which is ideally not distinguishable from real data.

The task of D is to classify the data as real or fake. The idea of GANs can be further extended, such that D has to identify the class label, if the sample is real, or to classify the sample as fake. In this architecture (SGAN) (Odena, 2016) the last layer of D is a softmax with $N+1$ output units representing the labels $\{class-1, class-2, ...class-N, fake\}$, where N is the number of different classes. Using this idea it was shown, that it is possible to train classifiers with higher accuracy, compared to conventional training. With fewer training data available, the better is the advantage of using the GANs.

The problem of this method is, that the retrieved classifier is not directly usable in real world environment, since it has learned the additional class $fake$, which does not exist in real world.

Using an auxiliary classifier GAN (AC-GAN) (Odena et al., 2016) it is possible to circumvent this problem. In the AC-GAN G takes an additional input, which determines the class of the fake sample. D has two different output layers. The first layer is a softmax with N units. G predicts a class label not only for real samples, but also for fake samples. The second output layer is a sigmoidal, which predicts if the sample is real or fake. The cost function therefore consists of two parts L_S and L_C.

$$L_S = \mathbb{E}[\log P(S = real \mid X_{real})] + \mathbb{E}[\log P(S = fake \mid X_{fake})] \quad (2)$$

$$L_C = \mathbb{E}[\log P(C = c \mid X_{real})] + \mathbb{E}[\log P(C = c \mid X_{fake})] \quad (3)$$

L_S corresponds to the log-likelihood of the correct source and L_C to the log-likelihood of the correct class. When training D the function $L_S + L_C$ is tried to maximize. G is trained to maximize the function $L_C - L_S$.

The advantage of this architecture is, that a classifier, which is fit for use in real world problems, can be directly retrieved from D. The only modification is to remove the sigmoidal output layer, which has to predict whether the sample is real or fake. Principally it is also possible to retrieve a useful classifier out of the SGAN architecture. In this case it is necessary to replace the last layers of D, which is the softmax layer with $N+1$ outputs, by a softmax layer with N outputs. Afterwards the last few layers of the network have to be retrained. Since this procedure seems to have no benefits, an AC-GAN is trained in order to improve the accuracy of the classifier.

3.3.1 Implementation

The discriminator has the same basic architecture as already shown in table 1. One change in the architecture was made by removing the last two layers. So the network firstly outputs a 1-dimensional feature vector. This vector is then inputed into two separate neural networks with two dense layers, which predict the class and the source of the sample. The ReLu nonlinearities have been replaced by Leaky ReLu‘s with slope 0.1. Since the whole network, when the generator is included, has increased in depth, it is feasible to use Leaky ReLu's in order to achieve good training results of the deep layers.

Another modification is, that the max-pooling layers have been removed. Since max-pooling would result in sparse gradients it would hinder the training process, especially of the generator. As a compensation the stride of the convolutional layers was changed to 2×2.

The architecture of the generator is shown in table 2. G takes two inputs, the class-input z_c and the noise-input z_n, and outputs one sample. z_n is a one-dimensional vector of size 100, drawn from a uniform distribution with values between 0 and 1. z_c is also a one-dimensional vector but with size 2. In order to connect z_n and z_c several possible solutions exist. In this work the connection between these two vectors is done via an element-wise multiplication.

Before it comes to the multiplication z_c is embedded, such that the dimension changes from 2 to 100. The embedding is done via a matrix with shape 2×100. The original vector z_c indicates which of the two vectors in the embedding matrix to choose. All values in the matrix are also learnable parameters.

Algorithm 1 : AC-GAN Training Procedure.

```
  Input: Number of iterations $I$ and batch size $m$
  for $i = 1$ to $I$ do
      Draw $m$ samples from real distribution.
      Update weights of $D$ with real samples.
      Draw $m$ random samples of $z_c$ and $z_n$.
      Update weights of $G$.
      Draw $m$ random samples of $z_c$ and $z_n$.
      Create $m$ synthetic samples.
      Update weights of $D$ with synthetic samples.
      Draw $m$ random samples of $z_c$ and $z_n$.
      Update weights of $G$.
  end for
```

Both the generator and the discriminator have been trained using the Adam optimizer with a decreased learning rate of 10^{-4}.

Algorithm 1 shows the procedure of one training step. The training procedure consists of overall four weight updates. Each G and D are both updated two times. The first update of D is done using real samples, whereas the second update is done using synthetic samples. G is updated both times in the same manner.

Figure 2 shows the validation loss for conventional and adversarial training. After 30.000 weight updates the method using adversarial training shows clearly better results. At the end of the training the adversarial method has a validation loss of 0.1 (binary accuracy of $95,1 \pm 1,7\,\%$) compared to a validation

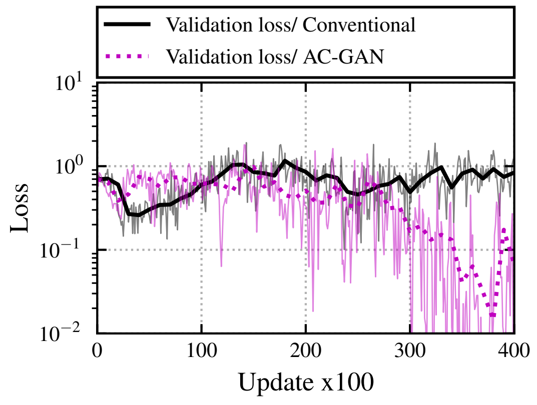

Figure 2: Comparison of learning curves between conventional and adversarial training.

loss of around 0.8 (binary accuracy of $80,1 \pm 2,5\,\%$) for non adversarial training. Using the adversarial method the discriminator sees more diverse sample and thus shows better generalization capability.

Figure 3 shows samples, which are synthesized by the generator, in comparison to real samples. The synthetic samples show a high similarity to the real samples.

3.3.2 Collapsing Generators

The results shown in figure 3 have been created with a collapsed generator. A collapsed generator means, that the G outputs the same image, regardless of the input. In the case of the AC-GAN architecture this means, that G collapsed to one fixed output for each class label. In literature feature matching (Salimans et al., 2016) is described as an effective way to prevent collapsing. When using feature matching the objective function of G is modified in a way that statistics of synthetic data matches statistics of the real data distribution. This is achieved by matching the activations of an intermediate layer of D for real and synthetic samples. In this work the activations of the last two dense layers before the final output are choosen to match. Since the architecture used in this work consists of two outputs $\{real?, label?\}$ feature matching is used for both outputs. Using this method resulted in no significant changes in both G and D. The evaluation accuracy remained mostly unchanged around $95\,\%$. The collapse of G could not be prevented.

Another approach to deal with collapsing generators is to directly target diversity of synthetic samples. Therefore the objective function of G is extended by the additional term 4 with $z_i = [z_{c_i}, z_{n_i}]$.

$$\mathbb{E}[||G(z_0) - G(z_1)||_2^2] \tag{4}$$

Table 2: Generator‘s architecture of the AC-GAN.

Operation	Kernel	Strides	Feature maps	BN?	Dropout	Nonlinearity
Class-input	N/A	N/A	N/A	N/A	N/A	N/A
Embedding	N/A	N/A	N/A	N/A	N/A	N/A
Noise-input	N/A	N/A	N/A	N/A	N/A	N/A
Multiplication	N/A	N/A	N/A	N/A	N/A	N/A
Dense	N/A	N/A	12288	$\surd$	$\times$	Leaky ReLu
Reshape	N/A	N/A	N/A	N/A	N/A	N/A
Upsampling	2×2	N/A	N/A	N/A	N/A	N/A
Convolution	3×3	1×1	32	$\surd$	$\times$	Leaky ReLu
Convolution	3×3	1×1	16	$\surd$	$\times$	Leaky ReLu
Convolution	3×3	1×1	16	$\times$	$\times$	Leaky ReLu
Convolution	3×3	1×1	1	$\times$	$\times$	Sigmoid

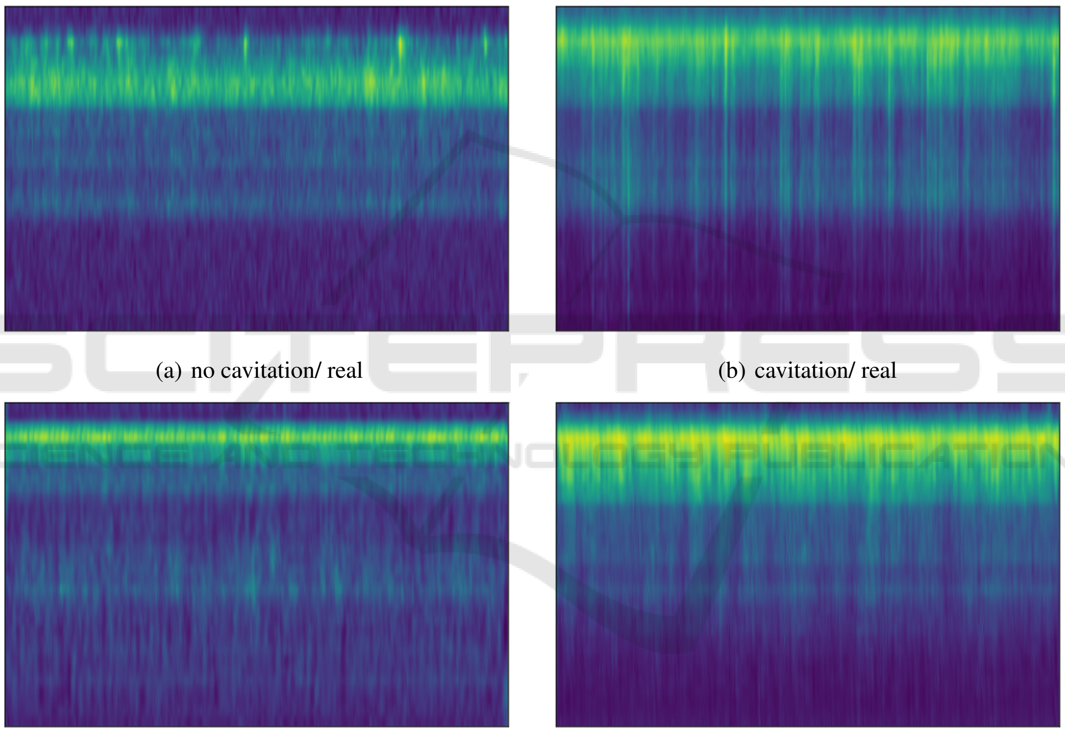
(a) no cavitation/ real (b) cavitation/ real

(c) no cavitation/ synthetic (d) cavitation/ synthetic

Figure 3: comparison between real and synthetic samples.

G is then trained to also maximize equation 4. In essence the pixelwise variance shall be maximized between two different inputs z_0, z_1 under the condition $z_0 \neq z_1$. In order to avoid cancellation between the new additional term and the original objective function G is trained in an alternating manner. Both terms are optimized independently from another. Using this modified objective function the resulting samples become very noisy and lack in dynamics (figure 4).

Since the euclidean distance depends on the absolute pixel value, high values will result in high penalization. Therefore G will avoid such high pixel values and the synthetic samples lack in dynamics.

The I-divergence represents an alternative to the euclidean distance. It is often used in the Nonnegative Matrix Factorization problem (Finesso and Spreij, 2004). The I-divergence for two nonnegative and two-dimensional samples X, Y is defined as:

$$D(X||Y) = \sum_{i,j} \left(x_{ij} \log \frac{x_{ij}}{y_{ij}} - x_{ij} + y_{ij} \right) \quad (5)$$

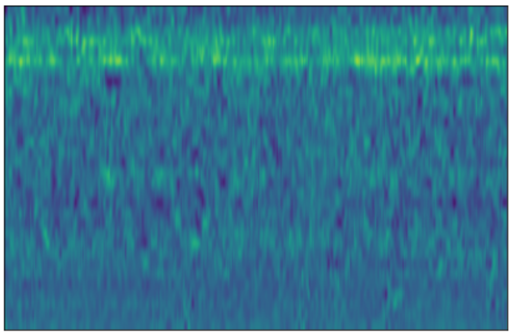

(a) cavitation/ sample 1

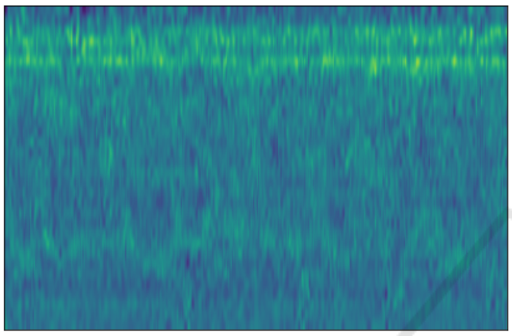

(b) cavitation/ sample 2

Figure 4: Synthetic samples using euclidean distance as additional term in the objective function.

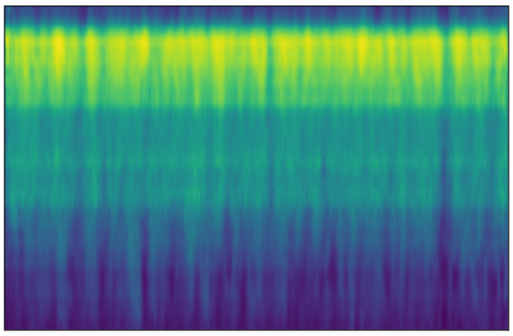

(a) cavitation/ sample 1

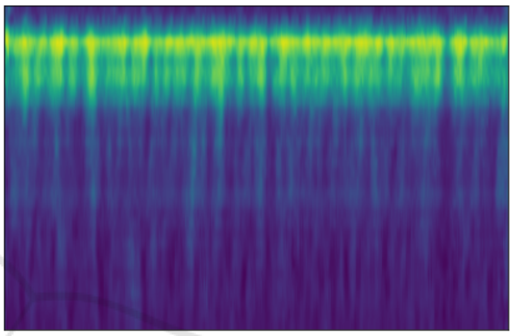

(b) cavitation/ sample 2

Figure 5: Synthetic samples using I-divergence as additional term in the objective function.

where x_{ij}, y_{ij} are the elements of X and Y. Like the euclidean distance the I-divergence is nonnegative and has the advantage that it is independent of the absolute pixel value. In order to avoid mathematical singularities X and Y are clipped between $[\varepsilon, 1]$, where ε represents a small number. The new additional term to the objective function of G is defined in equation 6.

$$\mathbb{E}[D(G(z_0)||G(z_1))] \tag{6}$$

Like before, this additional term shall be maximized and G is trained in an alternating manner. G did not collapse and the samples are looking realistic (figure 5). Nevertheless G did not learn the real data distribution. Several patterns resemble each other in sample 1 and 2. It seems that G learned few patterns and randomly varies the intensity of these. Although not learning the real data distribution, the evaluation accuracy could be raised to $98,1 \pm 1,2\,\%$.

Without wrapping the frequency axis experiments mostly resulted in no collapse of G. On the downside the evaluation accuracy dropped to $85\,\%$. Further investigations without wrapping have to be done before a final conclusion can be made.

4 SUMMARY AND OUTLOOK

In this work the usability of neural networks for detecting cavitation in hydraulic machinery was shown. Using a conventional CNN it was possible to achieve a binary classification accuracy of $94,2\,\%$. Utilizing GANs it was possible to push the classification accuracy to around $95,1\,\%$. Although the generator collapsed, an increase in accuracy was possible. Using the I-divergence as an additional term to the objective function resulted in more diverse synthetic samples and increased the accuracy to $98,1\,\%$. In further work the system shall be extended in such a way, that it becomes possible not only to detect cavitation, but also to distinguish between different cavitation types.

ACKNOWLEDGEMENTS

The research leading to the results presented in this paper is part of a common research project of the University of Stuttgart and Voith Hydro Holding GmbH. Also we want to thank Steffen Seitz from TU Dresden for the helpful exchange of ideas.

REFERENCES

Abadi, M., Agarwal, A., Barham, P., Brevdo, E., Chen, Z., Citro, C., Corrado, G. S., Davis, A., Dean, J., Devin, M., Ghemawat, S., Goodfellow, I., Harp, A., Irving, G., Isard, M., Jia, Y., Jozefowicz, R., Kaiser, L., Kudlur, M., Levenberg, J., Mané, D., Monga, R., Moore, S., Murray, D., Olah, C., Schuster, M., Shlens, J., Steiner, B., Sutskever, I., Talwar, K., Tucker, P., Vanhoucke, V., Vasudevan, V., Viégas, F., Vinyals, O., Warden, P., Wattenberg, M., Wicke, M., Yu, Y., and Zheng, X. (2015). Tensorflow: Large-scale machine learning on heterogeneous systems.

Escaler, X., Egusquiza, E., Farhat, M., Avellan, F., and Coussirat, M. (2006). Detection of cavitation in hydraulic turbines. *Mechanical systems and signal processing*, 20(4):983–1007.

Finesso, L. and Spreij, P. (2004). Nonnegative matrix factorization and i-divergence alternating minimization.

Gal, Y. and Ghahramani, Z. (2015). Dropout as a bayesian approximation: Representing model uncertainty in deep learning.

Goodfellow, I., Bengio, Y., and Courville, A. (2016). *Deep Learning*. MIT Press.

Goodfellow, I., Pouget-Abadie, J., Mirza, M., Xu, B., Warde-Farley, D., Ozair, S., Courville, A., and Bengio, Y. (2014). Generative adversarial networks.

Gregg, S., Steele, J., and Van Bossuyt, D. (2017). Machine learning: A tool for predicting cavitation erosion rates on turbine runners. *Hydro Review*, 36(3):28–36.

Ioffe, S. and Szegedy, S. (2015). Batch normalization: Accelerating deep network training by reducing internal covariate shift.

Koivula, T. (2000). On cavitation in fluid power. In *Proceedings of 1st FPNI-PhD Symposium*.

Lukic, Y., Vogt, C., Durr, O., and Stadelmann, T. (2016). Speaker identification and clustering using convolutional neural networks. In *IEEE International Conference on Acoustic, Speech and Signal Processing*.

Mesaros, A., Heittola, T., Diment, A., Elizalde, B., Shah, A., Vincent, E., Raj, B., and Virtanen, T. (2017). DCASE 2017 challenge setup: Tasks, datasets and baseline system. In *Proceedings of the Detection and Classification of Acoustic Scenes and Events 2017 Workshop (DCASE2017)*.

Odena, A. (2016). Semi-supervised learning with generative adversarial networks.

Odena, A., Olah, C., and Shlens, J. (2016). Conditional image synthesis with auxiliary classifier gans.

Sahidullah, M. and Saha, G. (2012). Design, analysis and experimental evaluation of block based transformation in mfcc computation for speaker recognition. *Speech Communication*, 54(4):543 – 565.

Salimans, T., Goodfellow, I., Zaremba, W., Cheung, V., Radford, A., and Chen, X. (2016). Improved techniques for training gans.

Schmidt, H., Kirschner, O., and Riedelbauch, S. (2014). Influence of the vibro-acoustic sensor position on cavitation. In *Proceedings of 27th Symposiom on Hydraulic Machinery and Systems*.

Srivastava, N., Hinton, G., Krizhevsky, A., Sutskever, I., and Salakhutdinov, R. (2014). Dropout: A simple way to prevent neural networks from overfitting. *Journal of Machine Learning Research*, 15:1929–1958.

Stowell, D., Wood, M., Stylianou, Y., and Glotin, H. (2016). Bird detection in audio: a survey and a challenge.

Zhao, R., Yan, R., Chen, Z., Mao, K., Wang, P., and Gao, R. (2016). Deep learning and its applications to machine health monitoring: A survey.